Northeast Atlantic and North Sea Storminess as Simulated by a Regional Climate Model during 1958–2001 and Comparison with Observations

Ralf Weisse, Hans von Storch, and Frauke Feser

GKSS Research Center Geesthacht, Institute for Coastal Research, Geesthacht, Germany

(Manuscript received 23 September 2003, in final form 19 July 2004)

ABSTRACT

An analysis of the storm climate of the northeast Atlantic and the North Sea as simulated by a regional climate model for the past 44 yr is presented. The model simulates the period 1958–2001 driven by the National Centers for Environmental Prediction–National Center for Atmospheric Research (NCEP–NCAR) reanalysis. Comparison with observations shows that the model is capable of reproducing impact-related storm indices such as the number of severe and moderate storms per year or the total number of storms and upper intra-annual percentiles of near-surface wind speed. The indices describe both the year-to-year variability of the frequency, as well as changes in the average intensity of storm events. Analysis of these indices reveals that the average number of storms per year has increased near the exit of the North Atlantic storm track and over the southern North Sea since the beginning of the simulation period (1958), but the increase has attenuated later over the North Sea and the average number of storms per year has been decreasing over the northeast Atlantic since about 1990–95. The frequency of the most severe storms follows a similar pattern over the northeast North Atlantic while too few severe storms occurred in other areas of the model domain, preventing a statistical analysis for these areas.

1. Introduction

Extratropical storms are a natural phenomenon that receives high public attention because of their high damage potential. Over the oceans, the high wind speeds associated with these events often cause extreme wave and surge conditions that, together with extreme wind speeds, may cause structural damages and thus represent potential hazards for shipping, fishing, offshore operations, and coastal protection, among others.

The question of whether the frequency or the intensity of extratropical storms may have changed within the past few decades and what such changes might look like, has been the subject of many investigations in the recent past (e.g., WASA Group 1998; Schmith et al. 1998; Alexandersson et al. 2000; Bromirski et al. 2003). Other authors focused on the changes to be expected in a future climate under changing atmospheric greenhouse gas concentrations (e.g., Beersma et al. 1997; Zwiers and Kharin 1998; Lionello et al. 2002; Geng and Sugi 2003). Considering the typical lifetimes of offshore structures or vessels in relation to the time scale for which a significant increase in atmospheric carbon dioxide concentrations is to be expected, such studies emphasize the importance for future planning purposes.

Extratropical storms are complex phenomena. Therefore, there are different analysis techniques that focus on different aspects of storm activity. For instance, studies concentrating on eddy growth rate (e.g., Hoskins and Valdes 1990) or bandpass-filtered variability (e.g., Blackmon 1976) focus more on the dynamical aspects of storm activity and generation. Studies analyzing storm surges (e.g., Flather and Smith 1998; Langenberg et al. 1999; Woodworth and Blackman 2002) or ocean wave heights (e.g., Günther et al. 1998; Vikebø et al. 2003) are more concerned with the impacts caused by severe storm events. Studies that [based on sea level pressure (SLP) maps] count the number of cyclones in an area using more or less sophisticated approaches usually focus mainly on changes in storm frequencies and/or changes in the core pressures of these cyclones (e.g., Zhang and Wang 1997; Simmonds and Keay 2000; Gulev et al. 2001). Analyzing changes in storm activity for the period 1949–99 using different techniques, Paciorek et al. (2002) concluded that, although there is some overall agreement in the results provided by the different approaches, regional details, and/or time behavior of the results obtained from the different approaches may vary significantly.

Corresponding author address: Ralf Weisse, GKSS Research Center Geesthacht, Institute for Coastal Research, Max-Planck-Strasse 1, D-21502 Geesthacht, Germany.
E-mail: weisse@gkss.de

For many practical applications impact-related measures are the most important. Wind speed would thus represent an optimal parameter for investigation as many hazards and damages are directly or indirectly (e.g., storm surges or extreme wave heights) related to it. However, when analyzing long-term changes in storminess, wind speed does not represent an optimal choice for several reasons: Wind speed observations that cover sufficiently long periods to allow the assessment of long-term changes and trends in storminess are only available at a few places. Often these measurements are affected by inhomogeneities, that is, they suffer from changes in instrumentation, measuring techniques, or changes in the surrounding of the station that may introduce spurious trends in the time series that are not related to changing storminess (e.g., WASA Group 1998). In addition, over the oceans, direct wind measurements are rare. Therefore, impact-related proxies such as geostrophic wind speed derived from station pressure observations (e.g., Schmidt and von Storch 1993) or, for the marine sector, storm surges (e.g., von Storch and Reichardt 1997; Woodworth and Blackman 2002), and wave heights (e.g., Kushnir 1997; WASA Group 1998) are frequently analyzed to assess long-term changes in storminess. For these proxies, longer and often more homogeneous time series are available than for wind speed. Other authors statistically combine wind speed measurements from periods that may be regarded as sufficiently homogeneous with large-scale data that are more homogeneously available for longer periods. An example of such an analysis is provided by Kaas et al. (1996) who used a statistical relationship between monthly means of SLP and wind speed observations at 10 northwestern European stations for the period 1961–87 to provide a reconstruction of the storm climate back to 1903. While this approach allows the reconstruction of local wind conditions for periods much longer than those for which direct (homogeneous) wind speed measurements are available, such reconstructions retain only that part of the variability that is controlled by the large-scale atmospheric circulation (e.g., von Storch 1999), while regional changes appear to be undetected. Therefore, attempts to provide gridded reconstructions of the wind (and wave) climate based on dynamical models have been increasing in recent years (e.g., Günther et al. 1998; Sterl et al. 1998; Cox and Swail 2001).

As mentioned earlier, direct wind measurements over the oceans are sparse. The situation improved when satellite data became routinely available and were assimilated in weather analyses. However, even weather analysis products are subject to a number of changes over time, such as changes in the numerical models and the data assimilation techniques used, or the day-by-day availability and quality of observational data. As for direct observations, these shortcomings may induce changes in the analysis products that are unrelated to changing weather conditions. To reduce these shortcomings, recently, so-called reanalyses projects have been initiated (e.g., Gibson et al. 1996; Kalnay et al. 1996). While little can be done to improve the quality, coverage, and resolution of the observational data used in the reanalysis, inhomogeneities related to changing analysis techniques are strongly reduced by using fixed state-of-the-art numerical models and data assimilation techniques.

Presently the longest reanalysis available is the one performed by the National Centers for Environmental Prediction–National Center for Atmospheric Research (NCEP–NCAR; Kalnay et al. 1996; Kistler et al. 2001). From this reanalysis, atmospheric data are available globally every 6 h for the period 1958–2002. The spatial resolution of these data is about 210 km $\times$ 210 km (T62). Recently, subsets of this reanalysis have been used to analyze changes in the storm climate. Examples are provided by Gulev et al. (2001), Harnik and Chang (2003), or Paciorek et al. (2002), and references herein.

Feser et al. (2001) have used the NCEP–NCAR reanalysis to drive a regional climate model (RCM) and performed a dynamical reconstruction of the atmospheric conditions from 1958 to 2001 at a resolution of about 50 km $\times$ 50 km. Their model domain covered Europe, the Baltic Sea, and the North Sea, together with the adjacent parts of the northeast North Atlantic. Compared to the driving NCEP–NCAR reanalysis, the enhancement in spatial resolution is about 1:16. Furthermore, the complete model output is also available at a very high temporal resolution (every hour), compared to the conventional 6-hourly interval at which operational analyses and reanalyses are usually provided. So far, all studies analyzing changes in storminess based on the NCEP–NCAR reanalysis data are subjected to the comparatively low resolution at which the reanalyses are run. In addition, most of these studies analyzed proxies for storminess (e.g., cyclone counts) that did not utilize near-surface wind speeds directly. Because of the high spatial and temporal resolution, as well as the availability of high-resolution gridded near-surface wind speed data, the simulation of Feser et al. (2001) presently comprises an optimal dataset to study and assess regional details of changing storminess over the past few decades. The latter is the purpose of this study. Our intention is twofold: First, we want to demonstrate that the model is indeed capable of reasonably simulating near-surface marine wind speed statistics that can be used to assess impact-related changes in storminess. Second, we want to analyze and assess the changes simulated by the RCM over the past few decades and examine the regional details of these changes.

The paper is structured as follows: Section 2 briefly describes the RCM and the simulation performed by Feser et al. (2001). In section 3, a brief description is provided of near-surface wind speed statistics that characterize the local storm climate and that are used in this study. In addition, we will compare these statistics with indices derived from direct wind speed measurements in order to demonstrate the extent to which the model is capable of simulating the statistics of extreme wind events (storms). Based on these wind speed statistics, the average storm climate of the simulation together with the changes that occurred over the past few decades are presented and discussed in section 4. Then in section 5 our results are summarized and discussed in relation to the findings of previous studies.

2. The RCM simulation: 1958–2001

We briefly describe the RCM simulation that has been performed by Feser et al. (2001) and from which the basic dataset for our analysis was obtained. The simulation was performed with the Regional Model (REMO) described in detail in Jacob and Podzun (1997) and Jacob et al. (1995). The model is based on primitive equations and is formulated for a gridpoint and terrain-following hybrid coordinate system. The prognostic variables are surface pressure, horizontal wind components, temperature, specific humidity, and cloud water. Furthermore, a soil model is included to account for variations in soil temperature and water content.

The experiment we analyze is a multidecadal REMO integration described in detail in Feser et al. (2001). The purpose of this integration was to provide a reconstruction of the regional atmospheric conditions during 1958–2001 for Europe and adjacent seas. In this integration, the model was forced by the NCEP–NCAR reanalysis. The NCEP–NCAR forcing was provided at eight grid points at the lateral boundaries using the classical approach described by Davies (1976). Additionally, the NCEP–NCAR large-scale circulation was forced upon the regional model using the spectral nudging approach suggested by von Storch et al. (2000). Spectral nudging may be seen as a suboptimal and indirect data assimilation technique (von Storch et al. 2000), depending on the quality of the global forcing fields. In case no further observations are available for assimilation into the regional model, spectral nudging can be considered as a simple approach to "assimilate" those scales of the global reanalysis in which we have the highest confidence. In other words, we would not like the regional model to *significantly* modify those scales that are reasonably resolved by the global reanalysis and that are supported by data assimilation. Weisse and Feser (2003) showed that the representation of extreme events in near-surface wind speed could indeed be improved in an RCM simulation when the spectral nudging approach was adopted. In the following, we will refer to a REMO setup utilizing the spectral nudging approach as SN-REMO.

The analyses presented in this paper are based on hourly near-surface wind speeds (10-m height above the surface) obtained from the described multidecadal regional atmospheric reconstruction. These data were available on a 50 km × 50 km grid covering Europe, the Baltic Sea, the North Sea, and adjacent parts of the northeast North Atlantic. The exact location and size of the model domain can be inferred from Fig. 1. Additionally, the locations of observing sites used for comparisons are indicated in Fig. 1. The comparisons are limited to stations in the North Sea. More comparisons of SN-REMO winds with observations in the Atlantic and the Mediterranean Sea can be found in García-Sotillo (2003) and Feser et al. (2003).

3. Comparison of near-surface wind speed statistics as derived from model simulation and from observations

a. Wind speed–based indices for storminess

The near-surface wind speeds obtained from the multidecadal simulation of Feser et al. (2001) can be con-

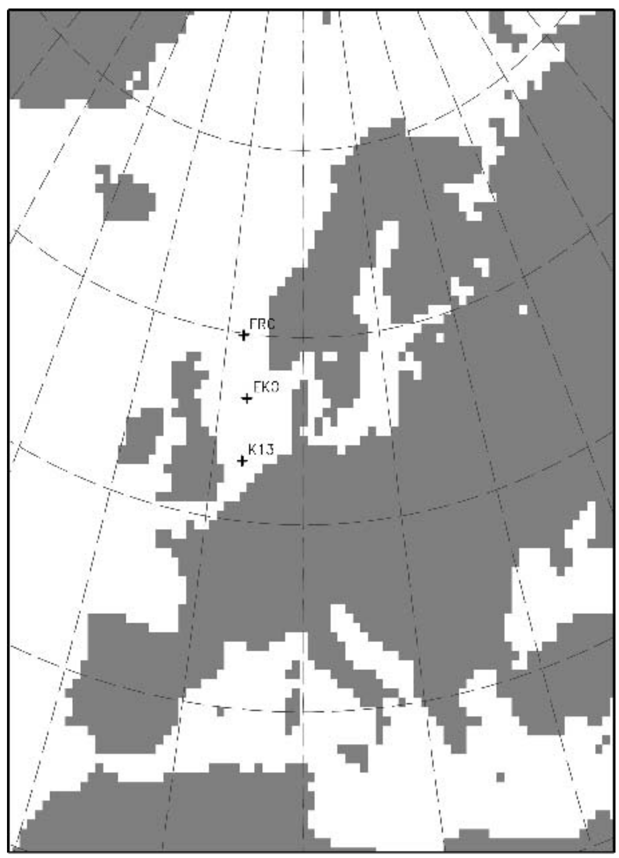

FIG. 1. The model domain used for the multidecadal SN-REMO integration. Land points are indicated in gray. The three crosses labeled FRG, EKO, and K13 show the locations of observing sites used for comparisons with the SN-REMO simulation.

sidered as relatively homogeneous.[1] In addition, they are available in gridded form at high spatial and temporal resolution (every hour). Thus, instead of adopting more frequently used approaches such as cyclone counts based on modeled surface pressures, we decided to analyze near-surface wind speeds directly. The high wind speeds usually associated with extratropical storms are directly linked to the potential hazards and damages that can be caused by a particular storm.

In many studies (mostly based on station data) intra-annual wind speed percentiles are chosen to assess changes in the storm climate within a particular area (e.g., Schmidt and von Storch 1993). Here, for instance, the 99th percentile denotes the wind speed that is (in a particular year) exceeded by only 1% of the observations. Thus an increase or a decrease in this wind speed percentile over several years provides an indication for a change in the storm climate. This change may be caused by more/less frequent or more/less violent storms or a combination of both.

To distinguish between both effects we chose a somewhat different definition: We identified a storm whenever the local near-surface instantaneous wind speed exceeded the threshold for Beaufort number (BFN) 8 (gale) on the Beaufort wind scale (17.2 m s^{-1}). We classified the event as a *moderate storm* whenever (based on hourly values) the highest wind speed that occurred during that event, remained smaller than BFN 10 (<24.5 m s^{-1}; Beaufort storm). Events with maximum wind speeds exceeding BFN 10 were classified as severe storms. According to this classification the total number of storms is the number of moderate storms plus the number of severe storms.

This storm counting has been performed separately at each model grid point. In order to analyze independent storm events, we further required that two storm events should be separated by at least 24 h, motivated by the average speed of low pressure systems at midlatitudes (e.g., Liljequist 1994). Storms were counted both annually and for the winter season only [December–January–February; (DJF)] Since our conclusions were not affected when changing from annual to seasonal storm counts, results for the annual counts are shown throughout the paper. Only in the section describing the relation with the large-scale atmospheric pressure field, will storm counts for the winter season be shown and discussed.

b. Comparison of model results with observations

For a number of marine stations, for which near-surface wind speed measurements were available, storm counts according to the definitions presented in the previous section have been determined and compared to those obtained from the RCM simulation. The result for Ekofisk, a platform located in the central North Sea, is shown in Fig. 2. In addition, comparisons of different intra-annual wind speed percentiles, as obtained from measurements and model simulation, are also shown. In general, all wind speed statistics show a reasonable agreement between observations and model results: Mean values as well as inter-annual variability of the different indices appear to be reasonably reproduced by the model. For the storm-count indices, a slight tendency toward an underestimation appears to occur for the number of total and moderate storms. Some of the differences between the model and observations can be explained by reduced data availability. When the model data are subsampled and analyzed only for those periods for which measurements have been available, the differences are reduced for some years indicating that measurements have failed in periods in which storms were present in the model. For Ekofisk, this is most obvious for 1983, while other years are less influenced by reduced data availability.

The number of severe storms at Ekofisk is remarkably small when derived from both observations and model simulation. During the entire 44-yr period not more than 4 severe storms per year have been identified for Ekofisk in the observations, and not more than 3 severe storms per year were found in the model results. Because of these small numbers, any systematic long-term change in the number of severe storms will be difficult to assess in a statistical sense. Severe storms are events with values far away from the mean and they are, by definition, less likely to occur. Any changes discussed here should therefore be considered with care. On the other hand, moderate storms are more frequent and assessing their changes therefore appears to be more robust.

Figure 3 shows the total number of storms and intra-annual wind speed percentiles for two more stations for which we have observational data. For K13-Alpha there is, again, reasonable agreement between the modeled and the observed storm indices. As for Ekofisk, the number of severe storms is relatively small (maximum 4 yr^{-1} in the observations and 2 yr^{-1} in the model run) and the model seems to slightly underestimate the number of total and moderate storms. The modeled wind speed percentiles show a rather good agreement with the observations. From about 1993 the number of storms, as well as the upper wind speed percentiles obtained from the observations, show a systematic decrease toward the end of the simulation period. This decrease could not, at least not in this strength, be obtained from the model data, resulting in larger discrepancies between observations and model-simulated storm indices at the end of the simulation period, in particular between 1998 and 2000. In 2001 the agreement between the modeled and the observed number of storms is again reasonable. In order to check whether

[1] They are homogeneous to the extent that the driving reanalysis can be considered homogeneous (see the introduction). No changes were applied to the model system during the integration.

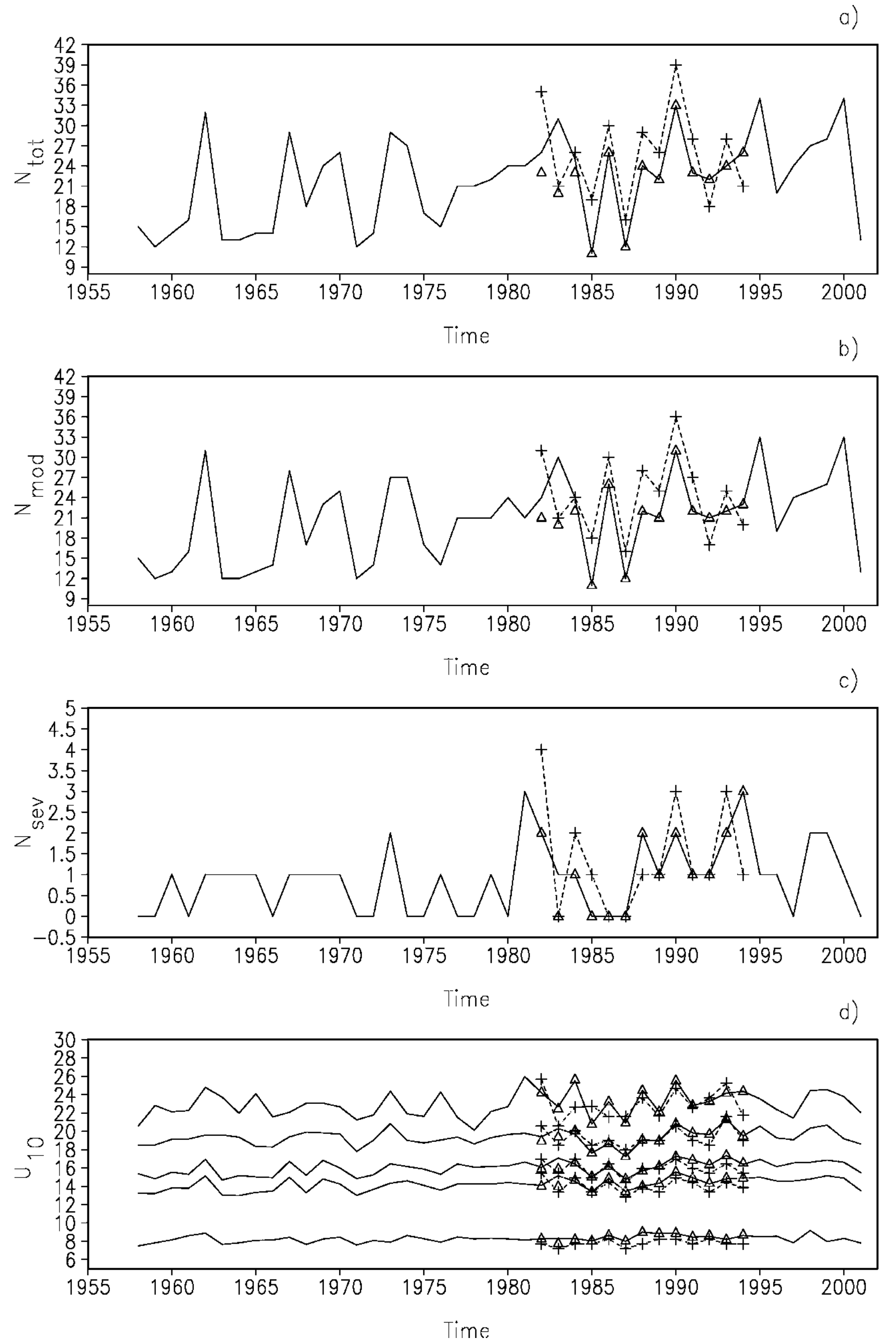

FIG. 2. Annual storm counts and intra-annual wind speed percentiles at the platform Ekofisk in the central North Sea (56.5°N, 3.2°E). (a) Total number of storms; (b) number of moderate storms; (c) number of severe storms; (d) (from bottom to top) intra-annual 50th, 90th, 95th, 99th, and 99.9th percentile of near-surface wind speed. Model results are shown as solid lines, and observations are shown as dashed lines marked with crosses. Triangles show results from subsampled model data taking only periods with available measurements into account.

this behavior is systematic, a similar analysis for Europlatform was performed. Europlatform is located approximately at 52°N, 3.28°E, not too remote from K13-Alpha. Again we found a good agreement between the modeled and observed storm indices. However, the results for Europlatform do not show any systematically increasing discrepancy between model values and observations toward the end of the simulation period (not shown) as it was described for K13-Alpha. We also compared model-derived wind speed statistics with

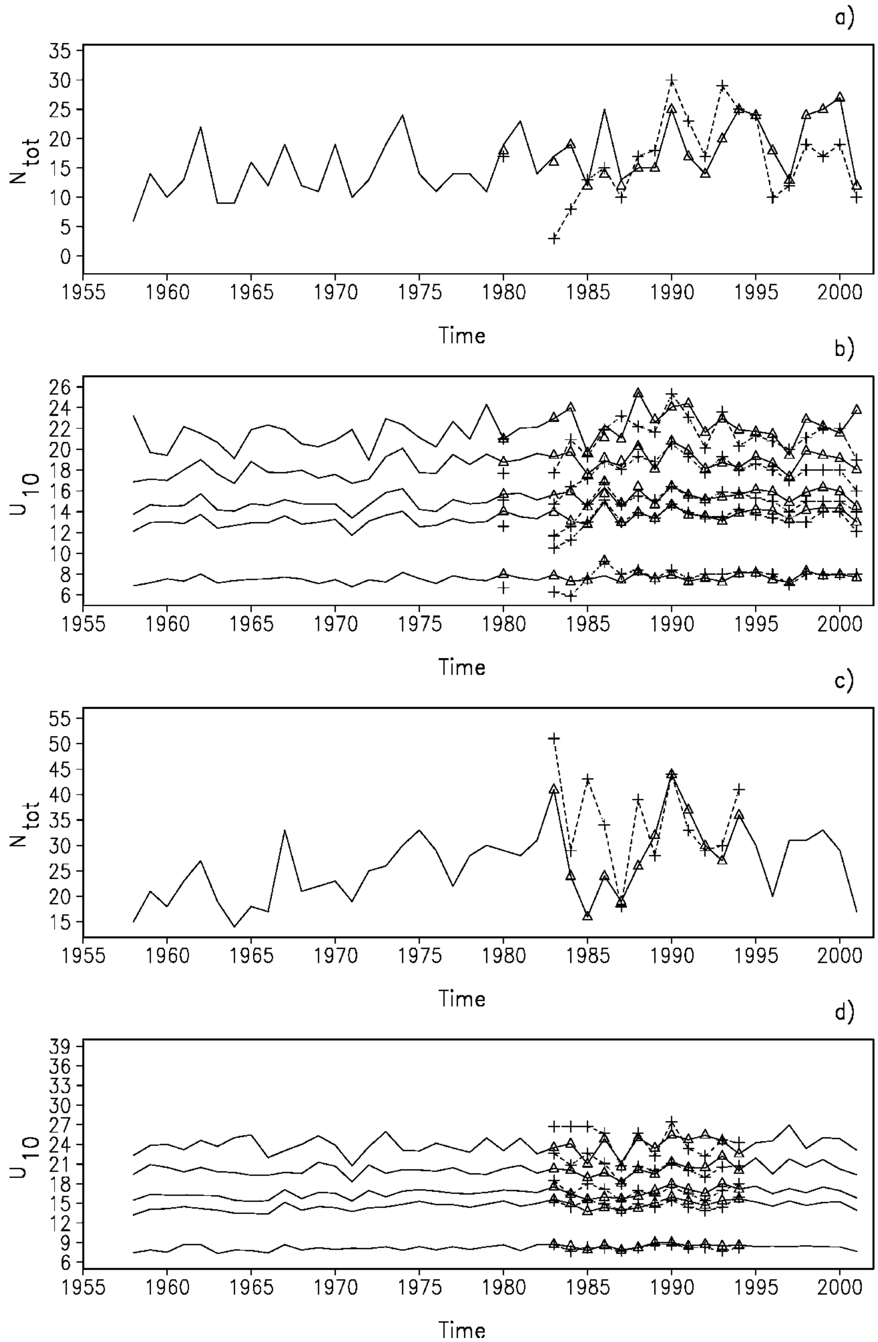

FIG. 3. (a), (c) Annual storm counts and (b), (d) intra-annual wind speed percentiles at the platforms (upper panels) K13-Alpha in the southern North Sea (53.22°N, 3.22°E) and (lower panels) Frigg (59.9°N, 2.1°E) northwest of Scotland. For each station the upper panel shows the total number of storms while the lower panel represents (from bottom to top) the intra-annual 50th, 90th, 95th, 99th, and 99.9th percentiles of wind speed. Model results are shown as solid lines, and observations are shown as dashed lines marked with crosses. Triangles show results from subsampled model data taking only periods with available measurements into account.

those based on measurements at Frigg (Fig. 3). Frigg is located at 59.9°N, 2.1°E, closer to North Atlantic storm track than the stations previously considered. Compared to the other stations, storms occur slightly more frequently at Frigg both in the observations and the model simulation. Again the agreement between wind speed statistics derived from the model and the observations appears to be reasonable.

Apart from the mentioned discrepancies we found, however, a good agreement between near-surface wind speed statistics obtained from model values and observations. Similar results have been reported recently also by García-Sotillo (2003) who compared observed near-surface marine wind speed statistics with those derived from a multidecadal SN-REMO simulation driven by the NCEP–NCAR reanalysis. García-Sotillo (2003) additionally showed that at buoys from which data had been assimilated into the reanalysis, no major differences occurred between observed wind speed statistics, those derived from the SN-REMO integration, and the statistics obtained directly from the reanalysis. However, when the comparison was made for buoys that had not been used for data assimilation, the SN-REMO simulation performed remarkably better. In particular, the statistics for high wind speeds improved significantly and, compared to the statistics obtained directly from the driving reanalysis, showed a much better agreement with observations. The latter demonstrates the extent to which, for marine wind speed statistics, added value can be obtained from a dynamical downscaling of the NCEP–NCAR reanalysis.

Recently wind fields from multidecadal SN-REMO simulations driven by NCEP–NCAR reanalysis data have also been used to drive ocean wave and storm surge models (e.g., Soares et al. 2002; Weisse et al. 2002). The results of these simulations show a good agreement with observations and may be considered as proxies for the quality of the driving wind fields.

Based on our own material and the evidence provided in the studies discussed above, we conclude that SN-REMO is capable of reasonably reproducing observed wind speed statistics, in particular, the average number of storms per year as well as their interannual variability. This conclusion is based solely on the comparison of model results with marine station data. Although we realize that land surface variables are relevant for many applications, we excluded land stations from the analysis for the following reasons: As in many other models, surface fluxes of momentum, heat, moisture, and cloud water are calculated from the Monin–Obukhov similarity theory with transfer coefficients depending on roughness length and Richardson number (Louis 1979). Over sea, the roughness is computed from the Charnock relation (Charnock 1955) modified after Miller et al. (1992). Over land, the roughness is a geographically prescribed function of vegetation and orography. As the terrain becomes increasingly complex, wind fields become more inhomogeneous, and a comparison of individual point measurements with model values, which represent an average value over a grid cell (here about 50 km $\times$ 50 km), appears to be not justified. Over land, modeled grid cell averages hardly exceed the threshold for BFN 8 (gale) for the entire simulation period. Therefore, land areas are excluded from the analysis. Over the oceans, however, wind fields are sufficiently homogeneous within a grid box to justify a direct comparison with measurements. Based on our analysis, the results provided by Feser et al. (2003) who concluded that the RCM simulation reasonably reproduces observed wind field variance even in the high-frequency range as well as on the results from García-Sotillo (2003) discussed above we assume that the model provides a reasonable representation of the marine storm climate also for those areas and periods for which no direct measurements were available for comparison. In the following section we will analyze gridded model results to provide a more comprehensive overview of the changes in storminess that occurred in the analyzed model period 1958–2001.

4. The average modeled storm climate and recent changes

a. The average storm climate

Based on the 44-yr period, 1958–2001, simulated with the regional model, the average number of storms per year at each wet grid point in the model domain has been computed. The highest storminess is associated with the exit of the North Atlantic storm track with a maximum found approximately south of Iceland (Fig. 4). Here, on average, more than 50 independent storm events per year with wind speeds exceeding BFN 7 do occur. From these roughly 50 events per year, approximately 12%–14% are classified as severe storms with maximum wind speeds exceeding BFN 10 (not shown). The remainder represents moderate storms with maximum wind speeds between BFN 8 and 10. The ratio between severe and moderate storms systematically decreases eastward and southward. Over the North Sea, on average, only one or two severe storms are found per year. South of about 45°N no severe storms were identified in the simulation.

b. Recent changes in storminess

1) TRENDS

In order to assess systematic changes in the frequency of moderate, severe, and the total number of storm events that may have occurred over the simulation period, linear trends have been computed. The result is shown for the total number of storms in Fig. 5. Considering the entire simulation period 1958–2001, an increase in storminess for most marine areas north of about 45°N was found with maxima located approximately south and north of Iceland, as well as near Scotland and off the Norwegian coast. Here, an average increase of about 0.3 storms per year was estimated, which means compared to the beginning of the simulation period on average about 13 more storms per year were identified at the end of the simulation period for

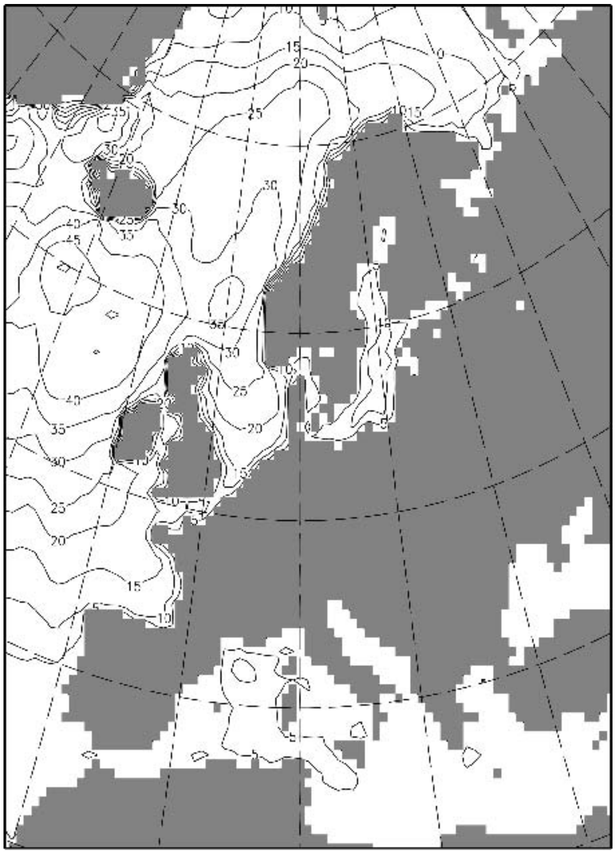

FIG. 4. Average number of independent storm events per year with maximum wind speeds exceeding 17.2 m s^{-1}. Contour lines are drawn for every 5 storms per year. For exact definitions see text.

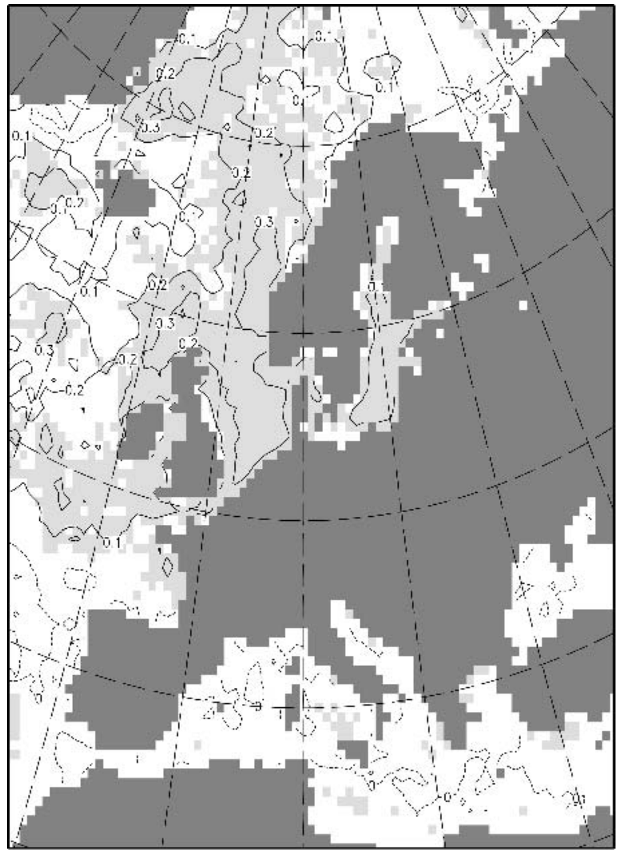

FIG. 5. Linear trend for the number of independent storms per year with maximum wind speeds exceeding 17.2 m s^{-1}. Contour lines show the trend 1958–2001 in number of storms per year. The zero contour line is dashed. Areas for which these trends are significantly different from zero at the 95% significance level are indicated by light gray shading. To assess the significance of the trends the Mann–Kendall test was applied to the prewhitened time series.

those regions. South of about 45°N, the pattern appears to be more noisy, providing indications of smaller and less systematic changes in the total number of storms. In addition, for some areas south of 45°N, a tendency toward decreasing storminess seems to exist (Fig. 5). The relative increase in storm frequency is strongest over the southern North Sea and the Baltic Sea where it reaches values of about 1%–2% yr^{-1} while for all other areas, changes are mostly less than 1% yr^{-1} (not shown).

For moderate storms the spatial pattern of the changes is rather similar (not shown). For severe storms the changes are more difficult to assess since these events are rare in the model simulation. Trends were therefore computed only for those grid points at which, on average, at least one severe storm per year occurred. The results of this computation indicate that the number of severe storms increased near the exit of the North Atlantic storm track by up to 0.1 storm per year, which corresponds to an increase of about 4 to 5 storms per year over the entire simulation period, or about 2% yr^{-1}.

In order to assess the significance of our results we tested whether the null-hypothesis trends not significantly different from zero could be rejected at the 5% significance level. The hypothesis was tested performing a Mann–Kendall test (Mann 1945; Kendall 1970) locally at each grid point. The test was applied to the prewhitened time series (Kulkarni and von Storch 1995) to account for the serial correlation present in the data. For the total number of storms, the result is shown in Fig. 5. It can be inferred that the changes north and south of Iceland as well as east of about 10°W, near Scotland, off the Norwegian coast, as well as over the North Sea and the Baltic Sea, appear to be significantly different from zero. For severe storms, only the changes in two small areas centered at about 57°N, 20°W and 65°N, 0° appear to be significantly different from zero (not shown).

The spatial patterns of the described changes bear some resemblance to those described in earlier studies. For instance, Günther et al. (1998) analyzed upper intra-annual wind speed percentiles derived from the weather analyses provided by the Norwegian Meteorological Institute. For the period 1955–94 these percentiles showed an increase between Iceland, Scotland, and off the Norwegian coast, as well as over the North Sea; while south of approximately 50°N, a decrease for some areas may be inferred.

2) Piecewise linear trends

While many studies have reported an increase in storminess since about 1960 or so over Europe and some of the adjacent marine areas (e.g., WASA Group 1998), indications do exist that the increase has weakened or even changed into a decrease in the last few years (e.g., Alexandersson et al. 2000; Schmidt 2001). In order to elaborate whether this is confirmed by our simulation and whether regional differences in these changes may be detected we slightly increased the complexity of the linear trend model applied in the previous section,

$$y_i = ax_i + b, \tag{1}$$

where y_i denotes the number of storms in year i, x denotes time, and a represents the linear trend. In this section, the model (1) was modified such that trends may change their amplitude and/or their sign once at a year T during the 1958–2001 simulation period,

$$a, b = \begin{cases} a_1, b_1 & : \quad i \le T \\ a_2, b_2 & : \quad i \ge T \end{cases}, \tag{2}$$

with the continuity condition that

$$a_1 x_T + b_1 = a_2 x_T + b_2. \tag{3}$$

We will refer to the results of this slightly more complex linear trend model as *piecewise linear trends.* It should be emphasized that the intention of this rather simple model is not to provide a perfect fit to the data. Rather the intention is to *slightly* increase the degrees of freedom and complexity of our statistical model in order to elaborate whether the linear trends in storminess described in the previous section can be considered as representative for the entire 1958–2001 period. Note that the year T at which trends may change their amplitudes and/or signs also represents a free parameter that is fitted to the data. It provides a rough indication at which times trends are most likely to have changed at individual grid points within our simulation period.

The piecewise linear trend model was fitted to the data locally at each grid point using a least squares method. The results of this exercise for the total number of storms are shown in Fig. 6. It can be inferred that the number of storms has increased at the beginning of the simulation period, in particular near the exit of the North Atlantic storm track and the southern North Sea. South of approximately 50°N, a decrease in storminess is obtained for some regions (Fig. 6a). However, this pattern does not remain constant for the 1958–2001 period but has changed considerably in later years for which a decrease in storminess is found near the exit of the storm track and off the Norwegian coast. Over the southern North Sea, the increase has weakened while south of about 50°N an increase in storminess may be inferred (Fig. 6b). The piecewise linear trend model suggests that over the northeast Atlantic, the change from an increasing trend toward a decreasing trend in storminess had occurred between about 1990 and 1995 (Fig. 6c). Over the North Sea, the spatial pattern of T is more noisy, indicating changes in trends between about 1962 and 1985. Over the Atlantic part of the model domain, the increase in storminess north of about 50°N at the beginning of the simulation period is accompanied by a corresponding decrease south of 50°N (Fig. 6a). This pattern changes toward the end of the simulation period when the number of storms increases south of and decreases north of about 50°N (Fig. 6b). This would be consistent with a north–south shift in the North Atlantic storm track.

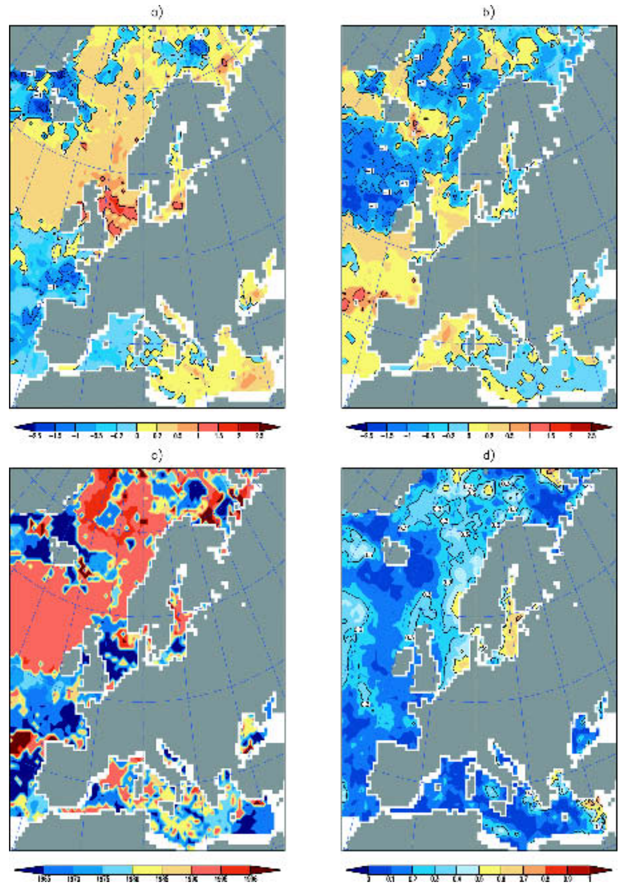

FIG. 6. Piecewise linear trends in the total number of storms per year with maximum wind speeds exceeding 17.2 m s^{-1}. (a) Linear trend a_1 for the 1958–T period; (b) linear trend a_2 for the T–2001 period. Units in both cases are number of storms per year. (c) Year T at which a change in trends is indicated by the statistical model. (d) Skill of the piecewise linear trend model with respect to a simple linear trend model. For exact definitions see text.

To test the extent to which this interpretation is influenced by the rather low storm activity in the last year of our dataset, the analysis was repeated discarding the year 2001. While the described patterns slightly change their amplitude at some places, their spatial structure and sign remained unchanged indicating that the interpretation of the results is not solely caused by low storm activities in 2001.

In order to test to what extent the piecewise linear trend model fits the data better than the simple linear trend model applied in the previous section, we computed the Brier skill score. The latter is defined (e.g., von Storch and Zwiers 1999) as

$$B = 1 - \sigma_F^2 \sigma_R^{-2}, \tag{4}$$

where σ_F^2 and σ_R^2 represent the error variances of the "forecast" F (in our case the one provided by the piecewise linear trend model) and the reference forecast R (provided by the simple time-independent linear trend model applied in the previous section). The error variances are computed relative to the same predictand which are the gridded total storm counts derived from the 44-yr SN-REMO simulation.

In our case, the Brier score provides a measure of the skill of the piecewise linear model relative to the simple linear time-independent model. Any positive value of B indicates that the piecewise linear trend model fits the data better than the time-independent linear trend model. Negative values would indicate a better performance of the reference. However, in our case, the Brier score cannot be smaller than zero. If the time-independent trend model would fit the data perfectly, the piecewise linear trend model would degenerate to $a_1 = a_2$ and $b_1 = b_2$, resulting in a Brier score of $B = 0$ as the smallest possible value. In our case the Brier score can be interpreted the following way: It may reach values between zero and one, measuring the improvement in fitting the data obtained from the piecewise linear trend model in percent relative to the time-independent linear trend model. The more the Brier score is different from zero, the larger the improvement obtained from the piecewise linear model, and the more inappropriate it is to assess changes in storminess from linear trends fitted over the 1958–2001 period.

The Brier score of the piecewise linear trend model relative to time-independent linear trends is shown in Fig. 6d for the total number of storms. It can be determined that the fit to the data is improved by about 10%–20% on the exit of the North Atlantic storm track and for large parts of the northeast Atlantic. This indicates that the total number of storms has indeed decreased in our simulation since about 1990–95. Over parts of the southern North Sea and the Baltic Sea, the Brier score reaches values of more than 50% indicating that for these areas, changes in trends have occurred in the 1958–2001 period. For moderate storms, the pattern is rather similar. For severe storms, our analysis indicates that on the exit of the North Atlantic storm track the number of severe storms has decreased since about 1990–95 while for other areas there were too few severe storm events to allow for a statistical analysis of the data.

3) Large-scale patterns and relation with the sea level pressure field

So far we have provided local analyses at each grid point. These analyses suggest that trends in storminess have changed their amplitude and/or sign during the 1958–2001 period. They further suggest, that these changes are not confined to smaller regions but obey some large-scale structure. In order to confirm this, we performed an empirical orthogonal function (EOF) analysis (e.g., von Storch and Zwiers 1999) of the total number of winter (DJF) storms (Fig. 7). The first EOF that explains roughly 45% of the total variance has a monopole structure with the highest amplitudes occurring near the exit of the North Atlantic storm track and off the Norwegian coast. This pattern closely resembles the average number of storms per year (Fig. 4). The principal component of the first EOF shows a behavior very similar to that obtained from the piecewise linear trend model. The storm activity was rather low at the beginning of the simulation period. Superimposed on strong fluctuations on a time scale of a few years, it increased from about 1975, reaching maximum values in the late 1980s and early 1990s from which it decreased again. At the end of the simulation period the storm activity is again at rather low levels. The principal components of higher EOFs do not show clear trends over the simulation period but pronounced interannual variability can be inferred (not shown).

In order to investigate how the variability in storm events relates to the dominant modes of large-scale atmospheric variability, we performed a canonical correlation analysis (CCA; e.g., von Storch and Zwiers 1999) between the total number of winter (DJF) storms and the mean SLP obtained from the SN-REMO simulation. The analysis is based on three EOFs for SLP and two EOFs for the storm counts. The first pair of canonical correlation patterns is shown in Fig. 8. For SLP, the pattern is characterized by a dipole structure with low pressure anomalies north of Iceland and high pressure anomalies over southwestern Europe, which closely resemble the North Atlantic Oscillation. In relation to this pattern, the number of storms is enhanced north of about 50°N with maximum values off the Norwegian coast near the exit of the North Atlantic storm track. The related time series share strong similarities with the first principal component for the total number of winter storms indicating a maximum in storm activity at the beginning of the 1990s with smaller values at the beginning and end of our simulation period.

Based on our results we conclude that the long-term variability in the number of extratropical storms in the

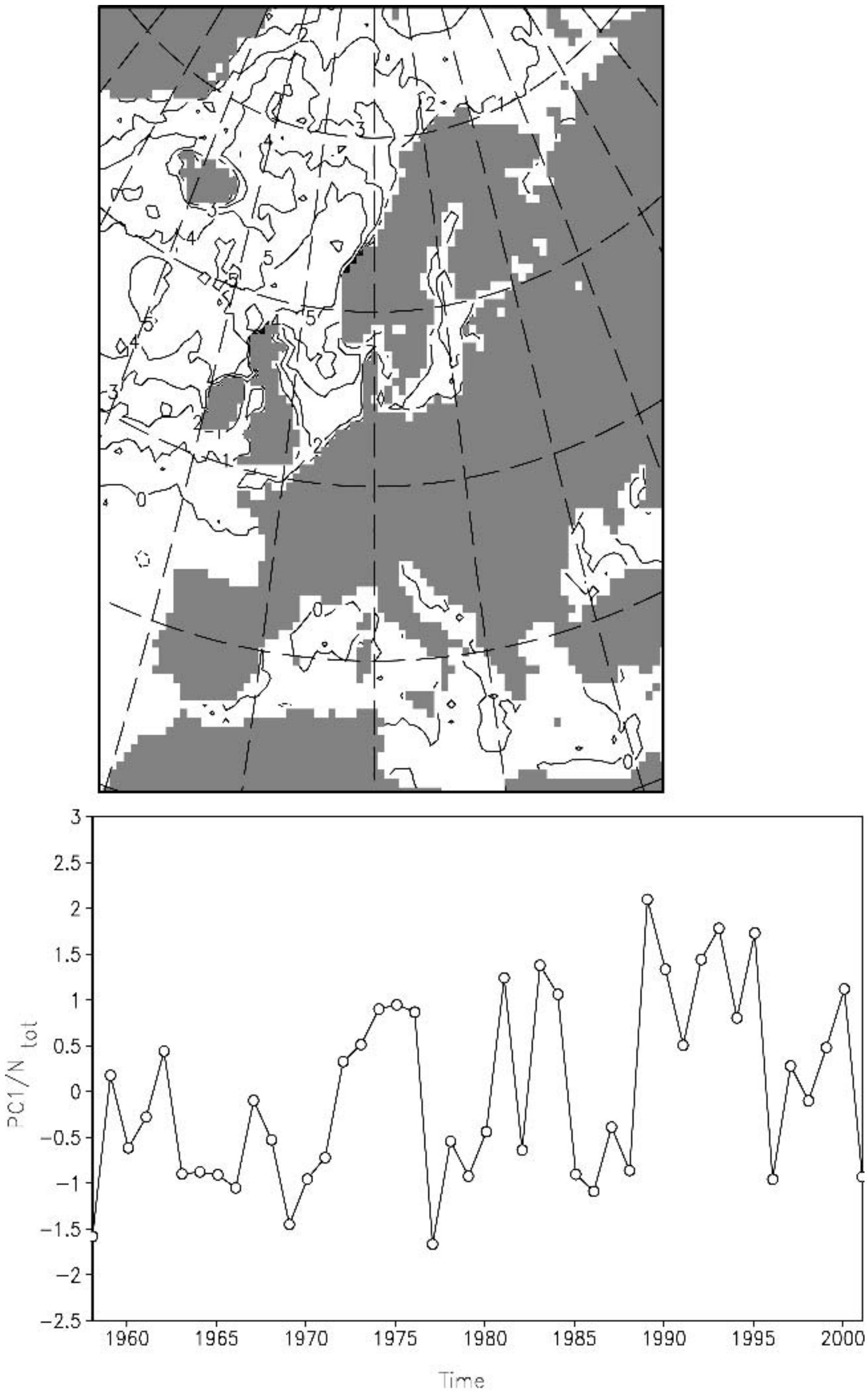

Fig. 7. (top) First EOF of the total number of winter storms per year and (bottom) the corresponding principal component.

1958–2001 SN-REMO simulation, in particular the increase since about 1975 and the subsequent decrease since the beginning of the 1990s, appears to be a large-scale phenomenon that is partly related to long-term fluctuations of the dominant modes of large-scale atmospheric variability.

5. Summary and discussion

Trends in severe weather are notoriously difficult to detect because of the relatively rare occurrence and the large spatial and temporal variability of these events (Houghton et al. 2001). Extreme events occur mostly

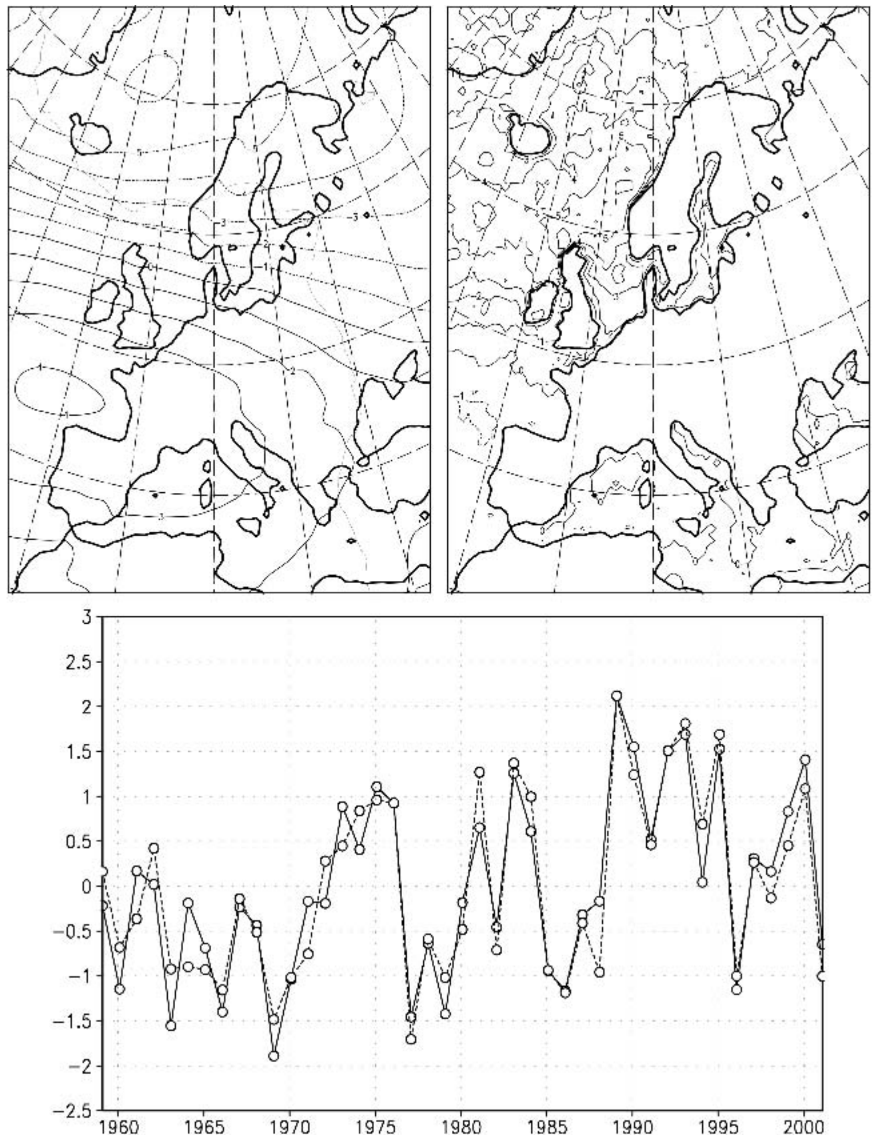

FIG. 8. (upper left) First pair of canonical correlation patterns for winter mean SLP and (upper right) the number of winter storms. The explained variances are 58% and 44%, respectively. (bottom) The related time series for the number of storms (solid) and SLP (dashed). The correlation is 0.94.

on the regional scale and have comparatively short lifetimes. The analysis of severe storm events requires long and homogeneous time series covering large areas at high spatial and temporal resolution. So far, this combination of data has not been available (Houghton et al. 2001).

In this study we analyzed wind fields obtained from a high-resolution regional climate model that was run for the 1958–2001 period. The model was driven by the NCEP–NCAR reanalysis and is thus expected to provide relatively homogeneous time series as inhomogeneities related to changing analysis techniques are strongly reduced in the driving reanalysis (Kalnay et al. 1996). In addition, wind fields from this regional simulation are available hourly, providing for the first time a spatially and temporal high-resolution homogeneous dataset that may be more suitable for the analysis of extreme storm events.

From this simulation, wind speed data at 10-m height above the surface have been used to derive several impact-related indices that describe the frequency and severity of storm events. In particular, the number of total, moderate, and severe storms as well as upper intraannual wind speed percentiles have been computed. Comparison of these indices with available station data revealed that the model is capable of reasonably simulating these indices. This conclusion is based on the comparison with data from marine stations. Comparisons for land stations have not been attempted because the model was run at a resolution of about 50 km $\times$ 50 km. Over the oceans, wind fields can be assumed to be relatively homogeneous over the area represented by one grid box and a comparison of model values (representing the average conditions over a grid cell) with measurements at an individual location appears to be justified. However, over land this assumption becomes more and more invalid as the complexity of the terrain increases.

Based on the finding that the model-simulated storm indices compared reasonably well with those obtained from observations at some marine locations for which measurements were available, we assumed that the model is also capable of reasonably simulating such indices for those marine areas for which no direct measurements were available. Based on this assumption we analyzed changes in storminess that occurred over the simulated 1958–2001 period. While linear trend analysis revealed an increase in storm frequency over most of the model domain north of approximately 45°N that was found to be significantly different from zero for most of the area east of about 10°W (Fig. 5), a more careful inspection revealed that the increase has weakened over the North Sea and has been replaced by a decrease in storm frequency over the northeast Atlantic north of about 50°N. Depending on the exact location, this change occurred between about 1990 and 1995 (Fig. 6). A similar result was found for the frequency of severe storms. Our EOF and CCA analyses further suggest that this pattern appears to be a large-scale phenomenon partly related to long-term fluctuations of the dominant modes of large-scale atmospheric variability. Considering the principal components of the EOFs only the first one (which accounts for about 45% of the total variance) shows an increasing trend until about 1990, followed by a subsequent decrease. The principal components of other EOFs do not show trends significantly different from zero.

Our findings are consistent with the results of other studies focusing on changing storminess for the same area. Variations on time scales of several decades have been documented for historical times (i.e., the seventeenth century) by De Kraker (1999) who studied reports about maintenance costs of Dutch dikes. For modern times, the WASA Group (1998) analyzed changes in the storm climate over the northeast Atlantic based on different datasets. Summarizing the findings from the different datasets, they concluded in 1998 that the storm climate over the northeast North Atlantic has undergone significant variations on time scales of decades; it has indeed roughened in recent decades (since about 1960–70) but the present storm climate (in 1995) was comparable to that observed at the beginning of the century (WASA Group 1998). This conclusion was to a large extent based on the findings of Alexandersson et al. (1998) who analyzed upper intra-annual geostrophic wind speed percentiles based on station pressure observations. Recently Alexandersson et al. (2000) provided an update of their analyses. Including more recent data, they showed that the storm activity has indeed decreased over the northeast Atlantic and the North Sea in the past few years.

In 1993, Schmidt and von Storch (1993) performed a similar analysis for geostrophic wind speed percentiles for the German Bight since 1876. Considering the entire period they found no significant trend in their data, although variations on the time scales of decades do exist and their time series shows pronounced minima around 1930 and 1970. An update of this analysis that now covers the period 1879–2000 confirms these findings (Schmidt 2001). The updated time series shows strong multidecadal fluctuations with maxima around 1920, 1950, and 1990, and also confirms the decrease in storm activity since about 1990–95 as obtained from our model simulation. In fact, from his analysis, Schmidt (2001) concludes that the last 5 yr (1996–2000) of his time series belong to the years that show the lowest storm activity of all within the century.

Harnik and Chang (2003) analyzed storm-track variations as seen in radiosonde observations and NCEP–NCAR reanalysis data. Although the signal was weaker in the radiosonde data, they found an intensification of the Atlantic storm track from the 1960s to the 1990s in both datasets. Jones et al. (1999) analyzed a gale index of geostrophic flow and vorticity for the United Kingdom for the 1881–1997 period. While they found an increase in severe gale days since about the 1960s, no significant long-term increase was found when the entire period was considered. Analysis of proxy data for storminess provides similar results. For instance, Woodworth and Blackman (2002) studied changes in extreme high waters at Liverpool for the 1768–1999 period. They concluded that their proxies pointed in particular to increased storminess during the late eighteenth and late twentieth centuries. For wave heights, a number of studies report increases over the past three decades but no longer-term trends are evident (Houghton et al. 2001).

To summarize, we conclude that marine surface wind fields are reasonably well simulated in the analyzed 44-yr RCM simulation (Feser et al. 2001). This allows for the assessment of changes in extreme wind conditions over the oceans for the past few decades. Based on these data, strong multidecadal fluctuations in storminess are found. The analysis of the most recent years of the simulation indicates that the increase in storminess at the beginning of the simulation period is replaced by a more moderate increase or even decreases for some areas within the last few years. This finding is consistent with more recent analyses of observational data. It is, however, difficult to speculate whether the decrease in storminess will continue within the next few years or whether a reintensification of extreme storm events might occur.

Acknowledgments. We thank Eduardo Zorita for his valuable technical help, in particular for providing us with his software for the EOF and CCA analyses. We also thank Magnar Reistad and Knut Iden from the Norwegian Meteorological Institute for their support and for providing us with data from Frigg and Ekofisk. The observational data for K13 were kindly provided by the Koninklijk Nederlands Meteorologisch Instituut (HYDRA project). This work has been financially supported by funding from the European Union under the Hindcast of Dynamic Processes of the Oceans and the Coastal Areas of Europe (HIPOCAS) project (Contract EVK2-CT-1999-00038).

REFERENCES

Alexandersson, H., T. Schmith, K. Iden, and H. Tuomenvirta, 1998: Long-term variations of the storm climate over NW Europe. *Global Atmos.–Ocean Syst.,* **6,** 97–120.

——, H. Tuomenvirta, T. Schmidth, and K. Iden, 2000: Trends of storms in NW Europe derived from an updated pressure data set. *Climate Res.,* **14,** 71–73.

Beersma, J., K. Rider, G. Komen, E. Kaas, and V. Kharin, 1997: An analysis of extratropical storms in the North Atlantic region as simulated in a control and a $2xCO_2$ time-slice experiment with a high-resolution atmospheric model. *Tellus,* **49A,** 347–361.

Blackmon, M., 1976: A climatological spectral study of the 500-mb geopotential height of the Northern Hemisphere. *J. Atmos. Sci.,* **33,** 1607–1623.

Bromirski, P., R. Flick, and D. R. Cayan, 2003: Storminess variability along the California coast: 1858–2000. *J. Climate,* **16,** 982–993.

Charnock, H., 1955: Wind stress on a water surface. *Quart. J. Roy. Meteor. Soc.,* **81,** 639–640.

Cox, A., and V. Swail, 2001: A global wave hindcast over the period 1958–1997: Validation and climate assessment. *J. Geophys. Res.,* **106,** 2313–2329.

Davies, H., 1976: A lateral boundary formulation for multi-level prediction models. *Quart. J. Roy. Meteor. Soc.,* **102,** 405–418.

De Kraker, A., 1999: A method to assess the impact of high tides, storms and storm surges as vital elements in climate history. The case of stormy weather and dikes in the northern part of Flanders. *Climate Change,* **43,** 287–302.

Feser, F., R. Weisse, and H. von Storch, 2001: Multi-decadal atmospheric modeling for Europe yields multi-purpose data. *Eos, Trans. Amer. Geophys. Union,* **82,** 305–310.

——, ——, ——, and E. Zorita, 2003: Comment on "Improved global maps and 54-year history of wind-work on ocean inertial motions" by M. H. Alford. *Geophys. Res. Lett.,* **30,** 2165, doi:10.1029/2003GL018026.

Flather, R., and J. Smith, 1998: First estimates of changes in extreme storm surge elevations due to the doubling of CO_2. *Global Atmos.–Ocean Syst.,* **6,** 193–208.

García-Sotillo, M., 2003: Reanálisis atmosférico pluridecenal de alta resolución en la cuenca Mediterránea. Ph.D. thesis, Universidad Complutense de Madrid, 216 pp. [Available from Universidad Complutense de Madrid, F. C. Físicas, Ciudad Universitaria, 28040 Madrid, Spain.]

Geng, Q., and M. Sugi, 2003: Possible change of extratropical cyclone activity due to enhanced greenhouse gases and sulfate aerosols—Study with a high-resolution AGCM. *J. Climate,* **16,** 2262–2274.

Gibson, R., P. Kålberg, and S. Uppala, 1996: The ECMWF reanalysis (ERA) project. *ECMWF Newsl.,* **73,** 7–17.

Gulev, S., O. Zolina, and S. Grigoriev, 2001: Extratropical cyclone variability in the Northern Hemisphere winter from the NCEP/NCAR reanalysis data. *Climate Dyn.,* **17,** 795–809.

Günther, H., W. Rosenthal, M. Stawarz, J. Carretero, M. Gomez, I. Lozano, O. Serrano, and M. Reistad, 1998: The wave climate of the Northeast Atlantic over the period 1955–1994: The WASA wave hindcast. *Global Atmos.–Ocean Syst.,* **6,** 121–164.

Harnik, N., and E. Chang, 2003: Storm track variations as seen in radiosonde observations and reanalysis data. *J. Climate,* **16,** 480–495.

Hoskins, B., and P. Valdes, 1990: On the existence of storm tracks. *J. Atmos. Sci.,* **47,** 1854–1864.

Houghton, J., Y. Ding, D. Griggs, M. Noguer, P. van der Linden, X. Dai, K. Maskell, and C. Johnson, Eds., 2001: *Climate Change 2001: The Scientific Basis.* Cambridge University Press, 881 pp.

Jacob, D., and R. Podzun, 1997: Sensitivity studies with the regional climate model REMO. *Meteor. Atmos. Phys.,* **63,** 119–129.

——, ——, and M. Claussen, 1995: REMO—A model for climate research and weather prediction. *Proc. Int. Workshop on Limited-Area and Variable Resolution Models,* Beijing, China, World Meteorological Organization, 273–278.

Jones, P., E. Horton, C. Folland, M. Hulme, D. Parker, and T. Basnett, 1999: The use of indices to identify changes in climatic extremes. *Climate Change,* **42,** 131–149.

Kaas, E., T. Li, and T. Schmith, 1996: Statistical hindcast of wind climatology in the North Atlantic and northwestern European region. *Climate Res.,* **7,** 97–110.

Kalnay, E., and Coauthors, 1996: The NCEP/NCAR 40-Year Reanalysis Project. *Bull. Amer. Meteor. Soc.,* **77,** 437–471.

Kendall, M., 1970: *Rank Corellation Methods.* 4th ed. Griffin, 258 pp.

Kistler, R., and Coauthors, 2001: The NCEP/NCAR 50-year reanalysis: Monthly means CD-ROM and documentation. *Bull. Amer. Meteor. Soc.,* **82,** 247–267.

Kulkarni, A., and H. von Storch, 1995: Monte Carlo experiments on the effect of serial correlation on the Mann-Kendall test of trend. *Meteor. Z.,* **4,** 82–85.

Kushnir, Y., 1997: The recent increase in North Atlantic wave heights. *J. Climate,* **10,** 2107–2113.

Langenberg, H., A. Pfizenmayer, H. von Storch, and J. Sündermann, 1999: Storm-related sea level variations along the North Sea coast: Natural variability and anthropogenic change. *Cont. Shelf Res.,* **19,** 821–842.

Liljequist, G., 1994: *Allgemeine Meteorologie.* Vieweg Verlagsgessellschaft mbH, 396 pp.

Lionello, P., F. Dalan, and E. Elvini, 2002: Cyclones in the Mediterranean region: The present and the doubled CO_2 climate scenarios. *Climate Res.,* **22,** 147–159.

Louis, J., 1979: A parametric model of vertical eddy fluxes in the atmosphere. *Bound.-Layer Meteor.,* **17,** 187–202.

Mann, H., 1945: Nonparametric test against trends. *Econometrica,* **13,** 245–259.

Miller, M., A. Beljaars, and T. Palmer, 1992: The sensitivity of the ECMWF model to the parameterization of evaporation from the tropical oceans. *J. Climate,* **5,** 418–434.

Paciorek, C., J. Risbey, V. Ventura, and R. Rosen, 2002: Multiple indices of Northern Hemisphere cyclone activity, winters 1949–99. *J. Climate,* **15,** 1573–1590.

Schmidt, H., 2001: Die Entwicklung der Sturmhäufigkeit in der Deutschen Bucht zwischen 1879 und 2000. *Klimastatusbericht 2001,* Deutscher Wetterdienst, 199–205.

——, and H. von Storch, 1993: German Bight storms analysed. *Nature,* **365,** 791.

Schmith, T., E. Kaas, and T. Li, 1998: Northeast Atlantic winter storminess 1875–1995 reanalysed. *Climate Dyn.,* **14,** 529–536.
Simmonds, I., and K. Keay, 2000: Variability of Southern Hemisphere extratropical cyclone behavior, 1958–1997. *J. Climate,* **13,** 550–561.
Soares, C., R. Weisse, J. Carretero, and E. Alvarez, 2002: A 40 year hindcast of wind, sea level and waves in European waters. *Proc. 21st Int. Conf. on Offshore Mechanics and Arctic Engineering,* Oslo, Norway, American Society of Mechanical Engineers, OMAE 2002-28604.
Sterl, A., G. Komen, and P. Cotton, 1998: Fifteen years of global wave hindcasts using winds from the European Centre for Medium-Range Weather Forecasts reanalysis: Validating the reanalyzed winds and assessing wave climate. *J. Geophys. Res.,* **103,** 5477–5492.
Vikebø, F., T. Furevik, G. Furnes, N. Kvamstø, and M. Reistad, 2003: Wave height variations in the North Sea and on the Norwegian Continental Shelf, 1881–1999. *Cont. Shelf Res.,* **23,** 251–263.
von Storch, H., 1999: The global and regional climate system. *Anthropogenic Climate Change,* H. von Storch and G. Flöser, Eds., Springer, 3–36.
——, and H. Reichardt, 1997: A scenario of storm surge statistics for the German Bight at the expected time of doubled atmospheric carbon dioxide concentration. *J. Climate,* **10,** 2653–2662.
——, and F. Zwiers, 1999: *Statistical Analysis in Climate Research.* Cambridge University Press, 494 pp.
——, H. Langenberg, and F. Feser, 2000: A spectral nudging technique for dynamical downscaling purposes. *Mon. Wea. Rev.,* **128,** 3664–3673.
WASA Group, 1998: Changing waves and storms in the Northeast Atlantic? *Bull. Amer. Meteor. Soc.,* **79,** 741–760.
Weisse, R., and F. Feser, 2003: Evaluation of a method to reduce uncertainty in wind hindcasts performed with regional atmosphere models. *Coastal Eng.,* **48,** 211–225.
——, ——, and H. Günther, 2002: A 40-year high-resolution wind and wave hindcast for the southern North Sea. *Seventh Int. Workshop on Wave Hindcasting and Forecasting,* Banff, AB, Canada, 97–104.
Woodworth, P., and D. Blackman, 2002: Changes in extreme high waters at Liverpool since 1768. *Int. J. Climatol.,* **22,** 697–714.
Zhang, Y., and W. Wang, 1997: Model-simulated northern winter cyclone activity under a greenhouse warming scenario. *J. Climate,* **10,** 1616–1634.
Zwiers, F., and V. Kharin, 1998: Changes in the extremes of the climate simulated by CCC GCM2 under CO_2 doubling. *J. Climate,* **11,** 2200–2222.